

Deciphering Structural Domains of Alkanethiol Self-Assembled Configurations by Friction Force Microscopy[†]

Carmen Munuera,[‡] Esther Barrena,[§] and Carmen Ocal^{*,‡}

Institut de Ciència de Materials de Barcelona, Consejo Superior de Investigaciones Científicas, Campus de la UAB, 08193 Bellaterra, Barcelona, Spain

Received: August 1, 2007; In Final Form: September 4, 2007

High resolution and high sensitivity friction force microscopy (FFM) is used to distinguish between different crystallographic domains of standing up molecular configurations of self-assembled alkanethiols partially covering Au(111) surfaces. We propose two suitable methods to decipher structural domains of the same configuration depending on the two-dimensional (2D) symmetry of the organic adlayer. For the hexagonal ($\sqrt{3} \times \sqrt{3}$)R30° where no differences among equivalent domains are expected in lattice-resolved scanning force imaging, different molecular domains however can be observed in lateral force images because of the friction asymmetry caused by domains presenting different relative orientations between the molecular tilt direction and the tip scanning direction. Since no lateral packing anisotropy is expected in this close-packed configuration, no friction anisotropy however is observed. Conversely, because of its rectangular space group symmetry, lattice resolved stick-slip imaging is enough to solve between the existing domains for the ($2 \times \sqrt{3}$) rectangular configuration.

Introduction

Although the term boundary lubrication was first used in 1922 to describe the regime in which very thin films, of molecular proportions, are effective in reducing the friction between solids in relative sliding motion,¹ it was the recent development of high-density storage technologies and micro- and nanomechanical systems what certainly revitalised the use of organic layers as protective/lubricant coatings. With the emergence of applications and devices relying upon nanotechnology, new materials are required to modify surface properties under severe space constraints, and therefore, lubricant films with monomolecular layer thickness are desired. Langmuir–Blodgett (LB) physical deposition and molecular self-assembly by chemical attachment of molecules to the surface are the two most common ways of creating these films. Because of their high hydrophobicity, low surface energies, and compact packing structure, these films usually have low adhesion and friction response which ensures minimal energy losses together with high wear resistance and stability within a wide range of experimental conditions. Therefore, the understanding of the molecular-scale tribological properties of organic films is crucial to modern technology. Since its invention in 1986,² the scanning force microscopy (SFM) has turned out as the suitable technique to address such investigations and study interfaces with molecular-scale sensitivity. On this scale, molecular properties such as local conformation, dispersion, packing arrangement, and chemical composition can directly influence the performance of the lubricant system.

The majority of the research on self-assembled monolayers (SAMs) has focused on alkanethiols on gold, with additional work on alkylsilanes on silicon oxide, and the aim of most of

the studies is to correlate the observed friction response with monolayer structures and seek possible energy dissipation processes during sliding.^{3–13} Frictional properties of these SAMs have been correlated with their chain length,^{5,7,14} including the effect of the pair-odd number of carbons within the chain,¹⁵ terminal group chemistry,^{16–18} or substrate nature.¹⁹ Friction is observed to increase as the adhesive interaction between the film surface and the SFM tip increases. The friction is also found to decrease with increasing chain length and remains almost constant beyond a certain critical chain length (approximately 10 carbons). These results point to a direct relationship between the lubricant efficiency and the monolayer packing density and are explained by the proposal that poor packing of the shorter molecules results in more energy dissipation modes (chain bending and tilting, rotations, formation of gauche defects, etc.), while these modes are sterically quenched in densely packed films formed by the longer chain molecules.^{5,17,20} The influence of packing disorder on friction has been also used to explain the higher frictional coefficient found in mixed SAMs, formed by co-adsorption of alkanethiol molecules with different chain lengths, when compared to single component SAMs. It was proposed that the greater disorder and higher concentration of gauche defects in mixed monolayers can raise their ability to dissipate energy during sliding.^{11,12,21}

On the other hand, it is well-established that when sliding a SFM tip over a periodic lattice, the so-called phenomenon of atomic stick-slip behavior yields lateral force images exhibiting the two-dimensional (2D) atomic or molecular periodicity of the surface under study. The explanation to this stick-slip behavior has been discussed in numerous experimental and theoretical works.^{4,22} It can be intuitively understood considering the combined action of the parabolic potential of the SFM tip (modeled as a spring) and of the periodically varying potential of the surface which results in a total potential that presents a series of local minima. At equilibrium, the tip resides in one local minimum. When the tip is pushed laterally, it will remain

[†] Part of the “Giacinto Scoles Festschrift”.

^{*} To whom correspondence may be addressed. E-mail: cocal@icmab.es.

[‡] Institut de Ciència de Materials de Barcelona.

[§] Present Address: Max-Planck-Institut für Metallforschung, Heisenbergstr. 3, 70569 Stuttgart, Germany.

at that minimum (“sticking”), until the restoring force of the cantilever is enough to overcome the energy barrier and effectively “un-stick” the cantilever, causing the tip to jump or slip to the nearest local equilibrium position, where it is locked again. At each jump from one minimum to the next, energy is dissipated, and lateral force images will indeed show the lattice periodicity of the surface. Though this is not true atomic resolution, these lattice-resolved images are extremely useful for surface structural characterization and, as we will show here, can be used to differentiate between coexisting domains of specific alkanethiol configurations where an accurate lattice orientation can be determined.

However, in practice, depending on the overlayer symmetry, this high-resolution imaging may not be enough to elucidate between coexisting domains. In such a case, other structural characteristics (such as tilt angle out of the surface normal, and tilt angle direction or azimuth) that might influence the frictional properties of molecular films could help visualizing, in friction force images, the coexistence of domains, otherwise not observed in topographic or lattice-resolved images. This would be, for instance, the case of friction anisotropy or friction asymmetry. Though both are related to the dependence of friction with the sliding direction, it is interesting to differentiate between both effects. The former refers to the variation of friction with the relative orientation angle between sliding surfaces or with the sliding direction itself. It is correlated with the relative crystallographic orientation of the sliding surfaces and the sliding direction (azimuthal dependence). A non-isotropic molecular packing would, for instance, produce such an effect. On the other hand, friction asymmetry refers to a change in friction when the sliding direction is changed by 180°. For the same relationship between the symmetry of the sliding surfaces, friction changes, when the sliding direction is reversed, are correlated to differences in molecular tilt out of the surface plane, that is, sliding direction parallel or antiparallel to the tilt angle direction.

Recently, friction anisotropy was reported in islands of oligothiophenes on mica and ascribed to domains with different molecular azimuth orientation relative to the scanning direction.²³ As a matter of fact, nearly one decade ago, lateral force microscopy measurements of thiolipid and polydiacetylene LB films on mica revealed the dependence of the friction on the molecular azimuth; that is, differences in the tilt angle direction of the molecules were revealed as contributing to a different torsion of the cantilever during forward and backward scans when scanning different domains coexisting in large molecular islands (as large as several microns).^{24–27} A lateral anisotropy in the packing of those films was proposed to be at the basis of this friction anisotropy.

Though it has been observed in some LBs^{24–26} and ferromagnetic materials surfaces,²⁸ despite the extensive number of SFM investigations of the $(\sqrt{3} \times \sqrt{3})R30^\circ$ ordered alkanethiols on gold, no friction asymmetry has been reported for this otherwise archetypal system. In this work, we present the first evidence of such an asymmetry caused by the out of plane molecular tilt dependence of friction in this system. This result helps us to decipher between equivalent domains of this structure, which due to their 2D hexagonal symmetry are not distinguished in high resolution (stick-slip) lateral force images.

On Au(111), the structure of the most stable alkanethiol phase consists of molecules with the sulfur end bound to the gold substrate and the alkane chains in an upright position forming a closely packed layer with $(\sqrt{3} \times \sqrt{3})R30^\circ$ periodicity.^{29–37} The alkane chains of the molecules are tilted at an angle of

approximately 30° from the surface normal, and regarding the tilt direction (i.e., the azimuth angle), it is commonly accepted as an average value the 14° away from the *NN* direction of the Au(111) (i.e., almost along the *NNN* molecular direction) reported in ref 31. Therefore, considering the 2D hexagonal symmetry of both the Au(111) substrate and the $(\sqrt{3} \times \sqrt{3})R30^\circ$ structure, 12 (if the small deviation from the *NNN* direction is neglected) equivalent molecular domains can coexist in a given substrate terrace when the tilt direction is considered. However, these domains cannot be distinguished neither from topographic SFM images (the thickness of the layer is the same regardless the tilt direction) nor in lattice-resolved images, since the SFM is “blind” to this azimuth angle. In this study, we show that, conversely to topographic and high-resolution stick-slip SFM imaging, high sensitivity lateral force images can be used to resolve these otherwise undistinguishable structural domains. These domains are obtained after mild annealing of samples consisting of islands of alkanethiol molecules self-assembled on Au(111) which were previously obtained as described elsewhere.³⁸ The domain lateral size is 1 order of magnitude smaller than those reported in thiolipid LB films. The presented results confirm the influence of the tilt direction on the frictional properties also in alkanethiol SAMs at the nanometer scale.

In addition to that and thanks to our preparation procedure³⁹ we are able to also obtain alkanethiol islands presenting a rectangular $(2 \times \sqrt{3})$ rect structure, commensurate with the underlying substrate.^{39–41} In these islands, the alkane chains are tilted 50° with respect to the surface normal, with an average azimuth angle 48° from the *NN* molecular direction. Conversely to what happens with the hexagonal configuration, because of the different 2D symmetry of the rectangular adlayer with respect to the Au(111) substrate, the symmetry is broken and three differently oriented domains should be distinguished in lattice-resolved SFM images. Strong evidence is provided by resolving such domains coexisting in a given island. We emphasize the importance of the use of partially uncovered surfaces (submonolayer coverage) in which the bare substrate areas serve as lattice periodicity and accurate lattice orientation reference.

Experimental Section

Sample Preparation. The gold substrates (200–300 nm Au/1–4 nm Cr/glass, from Arrandee) were cleaned by immersion in a piranha solution (1:3, H₂O₂:H₂SO₄) for some minutes followed by flame annealing. This procedure resulted in surfaces consisting of large grains with flat terraces of (111) orientation (sizes up to 400 nm) separated by monatomic steps. Flatness and cleanness were tested by the quality of the lattice-resolved SFM images of the gold substrate. The alkanethiol molecules employed in this study were dodecanethiol (C₁₂H₂₅SH, C12) and octadecanethiol (C₁₈H₃₇SH, C18) from Aldrich Chemical Company and were used as received, without further purification. Islands of self-assembled molecules were prepared at room temperature ($\approx 21–25$ °C) by immersing the gold substrates in very dilute (< 0.5 μ M) ethanol solutions of the corresponding molecule for time periods of 10–50s. Afterward, the samples were rinsed with absolute ethanol and dried under a N₂ stream to remove weakly adsorbed molecules. This procedure led to the formation of alkylthiol islands with various sizes and morphologies. Depending on precise preparation parameters, that is, particular combinations of molecular concentration, immersion time, and temperature, two differently tilted configurations of upright molecules can be obtained and, in some cases, coexist. The molecular order of these configurations, the hexagonal $(\sqrt{3}$

$\times \sqrt{3}R30^\circ$ of the monolayer and a rectangular ($2 \times \sqrt{3}$) rect phase, has already been reported.^{39,40} In the present investigation, after substrate withdrawal from solution, some samples have been annealed at 70 °C during 20 min, under ambient conditions, whereas others have been allowed to evolve at ambient temperature. As it will be shown, the annealing procedure facilitates the coalescence of differently tilted domains, which are not observed in the case of slow room-temperature diffusion, where large single domain islands are obtained.⁴²

Scanning Force Microscopy. Normal-force and lateral-force measurements have been performed, under ambient conditions, on a homemade microscope head combined with an SPM100 control unit and software from Nanotec Electrónica.^{43,44} Sharpened, V-shaped, Si₃Ni₄ cantilevers (Park Scientific Instruments) with nominal force constants of $k = 0.50$ N/m were used in this study. Normal and torsional deflections of the cantilever were simultaneously measured by means of a four-quadrant photodiode. The voltage difference of the upper and lower segments is proportional to the normal deflection of the cantilever and consequently related to the sample topography. The voltage range between the right and the left segments is proportional to the torsion of the cantilever which is a direct measure of the lateral force and related to friction. Forward (scanning from left to right) and backward (scanning from right to left) lateral force images are always recorded.

Results and Discussion

By varying the employed conditions (concentration, temperature, immersion time), our preparation procedure, based on the use of submonolayer coverages, leads to the formation of islands presenting either the hexagonal ($\sqrt{3} \times \sqrt{3}R30^\circ$) structure of the monolayer or a rectangular ($2 \times \sqrt{3}$) rect structure, also commensurate with the underlying substrate, with the alkane chains tilted 50° with respect to the surface normal. We always resort to topographic images (the difference in tilt angle values yields different island's thickness) and lattice-resolve SFM images to ascertain the actual configuration of a given island. As reported previously,^{40,41} both molecular tilts (30° and 50°) can be obtained for a wide series of molecular lengths, and the results presented here are not chain length dependent. Data obtained for two different alkanethiol molecules (C18 and C12) are used to illustrate our discussion.

In the case of the rectangular configuration, lattice-resolved images can be employed to reveal the coexistence of different molecular domains within a given island. Figure 1 shows an example of one island formed by two such equivalent rectangular domains. Apart from determining the relative orientation of the domains, their molecular periodicity and lattice orientation are determined by using high-resolution images of the surrounding Au(111) bare terraces.

The topographic image in Figure 1a shows two C18 islands almost covering the gold terraces underneath. Because of a high local coverage in this area, and as it is common in the case of complete monolayers, different structural defects (vacancies, pinholes, etc.) are observed. In particular, we highlight by an arrow the presence of a domain boundary. From lattice-resolved images, we know that the islands present the rectangular configuration with lattice parameters 0.49 nm \times 0.58 nm and a 50° molecular tilt. The high-resolution image (b), taken at the marked area in (a), proves that the boundary is formed by the coalescence of neighboring growing domains, which present different orientations within the same island. Two ($2 \times \sqrt{3}$) rect equivalent lattices, rotated 30°, are clearly resolved. On the basis of the relative orientation between both and between

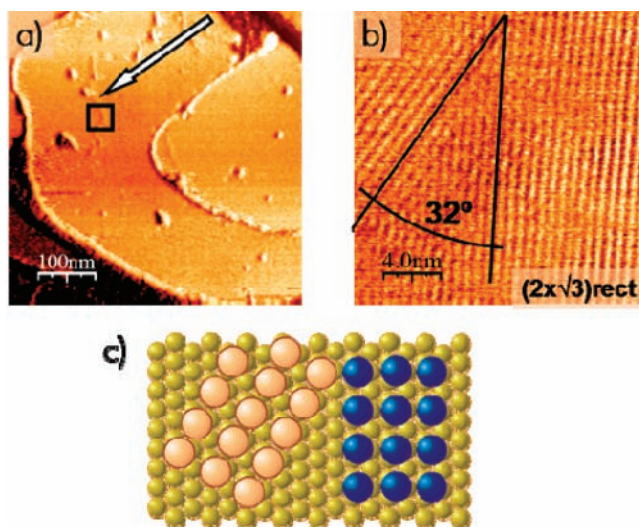


Figure 1. (a) Topographic image of a C18 sample. The white arrow indicates the presence of a domain boundary. (b) Lattice-resolved lateral force image taken in the area marked in (a) to show the coexistence of two ($2 \times \sqrt{3}$) rect domains, 30° rotated. (c) Schematic model of the rectangular domains observed in (b). Small circles correspond to the Au(111) lattice, whereas large circles represent the molecular periodicity (only end groups are depicted for simplicity). Total z scale: (a) 0–2.5 nm.

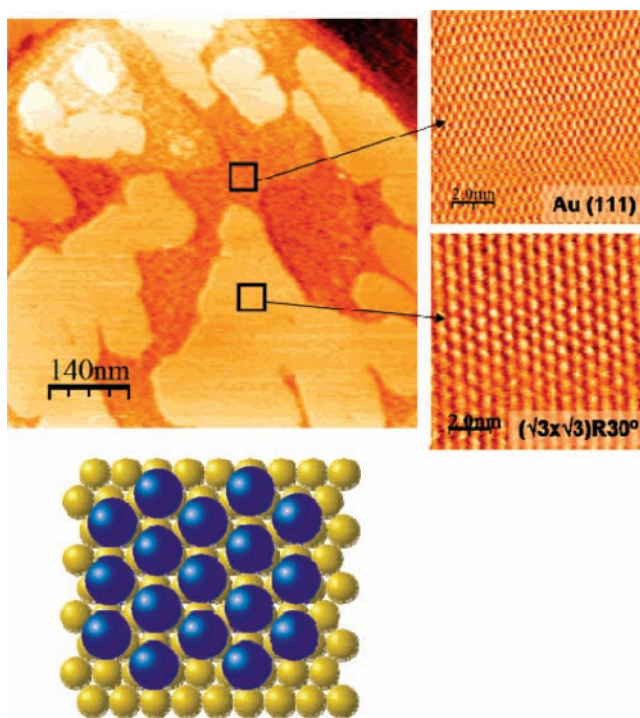


Figure 2. Top: topographic image of a C12 sample. Total z scale: 0–3 nm. Lattice-resolved lateral force images on the Au(111) (top right) and C12 island (bottom right) show that the molecules are arranged in the hexagonal ($\sqrt{3} \times \sqrt{3}R30^\circ$) configuration, commensurate with the underlying substrate. Bottom: schematic model showing the 2D molecular arrangement.

each domain and the underlying substrate (lattice-resolved images of the underneath gold terraces were also obtained), we can figure out the most likely molecular order, which has been schematically depicted in (c).

Figure 2 shows the topographic image of a C12 sample consisting of islands with a height that corresponds to molecules in a configuration with a tilt angle of 30°. Lattice-resolved images measured on the Au (111) terrace (top right image) and

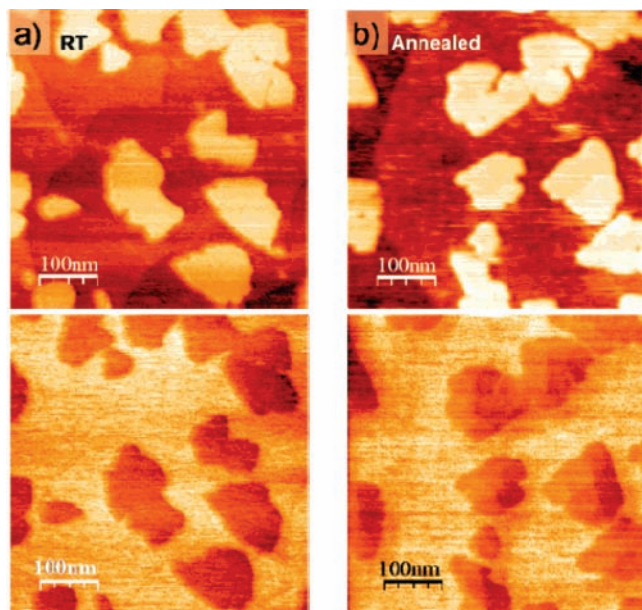


Figure 3. Topographic (top) and lateral force (bottom) images of C12 samples. The sample in (a) was allowed to evolve at room temperature (RT), after substrate withdrawal from solution, whereas the sample in (b) was submitted to mild annealing after preparation.

on top of the islands (bottom right image) confirm that the molecules are arranged in the $(\sqrt{3} \times \sqrt{3})R30^\circ$ hexagonal structure. The schematic model shown at the bottom of the image represents the 2D molecular arrangement. On the basis of combined SFM and GIXRD experiments,⁴⁵ we know that these hexagonal islands are usually single structural domains formed after a slow ripening process (lasting hours at room temperature) driven by long-range surface diffusion and molecular rearrangement. Obviously, different islands may present different rotational domains. However, converse to what happens with the rectangular configuration, different $(\sqrt{3} \times \sqrt{3})R30^\circ$ domains will appear identical in lattice-resolved SFM images.

Since, in this work, we are interested on deciphering between coexisting equivalent structural domains, we promoted a defective molecular self-assembling by annealing at 70 °C during 20 min. This procedure enhances surface molecular diffusion, and as a consequence, structural domain coalescence is expected to occur. Unfortunately, elucidating if more than one equivalent domains are present remains hindered in lattice-resolved SFM images. A different approach is needed, and as we show below, the coexistence of domains in islands arranged in the hexagonal configuration can only be discerned in lateral force images comprising the whole island.

The results are illustrated in a comparative way in Figure 3, where the simultaneously acquired topographic (top) and lateral force images (bottom) of two C12 samples are presented. After withdrawal from solution, sample a was allowed to evolve under ambient conditions, whereas sample b was annealed at 70 °C for 20 min. In both cases, the measurements were performed several hours after sample preparation.

The topographic images show negligible differences between both samples: they consist of islands of 50–150 nm diameter coexisting with bare gold terraces. As proven in previous works,^{9,39–41} our preparation procedure leading to submonolayer coverages is a very convenient approach to obtain accurate height values, since the presence of bare flat Au(111) terraces serve as an excellent in situ reference to measure the film thickness. In both samples, all of the islands show a very

uniform topmost surface with less than 0.03 nm height differences over the whole island area.

Lattice-resolved images like those shown in the previous figure were acquired, all of them exhibiting the hexagonal $(\sqrt{3} \times \sqrt{3})R30^\circ$ periodicity, regardless of the preparation temperature used. However, large area lateral force images (bottom images in Figure 3) clearly show some noticeable differences between annealed and non-annealed samples. In these images (for simplicity only forward lateral force images are shown), the color code is such that brighter (darker) areas correspond to higher (lower) values, and therefore, the alkanethiol islands appear as dark patches. Islands on the non-annealed sample, where single domain islands are expected to form, do present a uniform signal all over their surface (bottom left image). Conversely, in the annealed sample, areas presenting different lateral force contrast are clearly resolved within each individual island (bottom right image), indicating the existence of different domains. Since these domains are observed for the same island height in the annealed sample, we suggest that the molecules forming these islands might present different orientations relative to the scanning direction.

In order to make clearer the above observation, Figure 4 shows a close-up of one of the annealed islands. The topographic image in part a reveals an extremely flat island, as seen in the topographic profile taken across it and, more clearly, in the line scan restricted to the very island top, which shows fluctuations smaller than 0.03 nm. This is only consistent if a unique molecular tilt angle exists throughout the whole island.

More detailed analysis in terms of friction can be performed. In part b, we show forward and backward lateral force images simultaneously acquired. Four different domains meeting at the center of the island and presenting different frictional contrast can clearly be distinguished. Two of them (upper and lower ones) exhibiting a fairly similar contrast are confined by an $\approx 60^\circ$ angle. The other two (right and left ones) are confined by $\approx 120^\circ$ angles. The bottom graph presents the forward (black) and backward (gray) lateral force signal along the scan lines marked in the corresponding images. These profiles cross domains labeled 2, 3, and 4 as well as the bare gold terrace. The lateral force signal measured on the Au(111) substrate is taken as a reference.

Taking into account that the lateral force signal (measured as the cantilever torsion) is opposite for reversed scan directions, that is, larger lateral forces are visualized as bright colors in the forward scans whereas larger lateral forces are seen as darker colors in the backward profiles, and using the gold back and forth signals to establish the zero as an accurate reference, we observe that the lateral force is asymmetric and that the cantilever lateral torsion changes within a given domain when the sliding direction is changed by 180° (i.e., from back to forth). This can be checked, for example, by comparing domains 2 and 4 in the bottom graph of Figure 4: in the forward scan profile, domain 2 exhibits a lower lateral force signal than domain 4; when the scan is reversed, domain 2 exhibits a higher lateral force signal than domain 4. A different tilt angle direction within the domains is at the origin of this asymmetry.

Remarkably, these differences in the lateral force profiles do not lead to differences in the calculated friction for the observed domains. As it is known,⁴ the total friction within an area of homogeneous characteristics is calculated as $1/2(F_1^f - F_1^b)$ where F_1^i is the lateral force signal along that line in the forward ($i = f$) and backward ($i = b$) scan. Data in Figure 5 correspond to the calculated friction force along the scan line marked in Figure 4. The three domains (2, 3, and 4) present the same friction

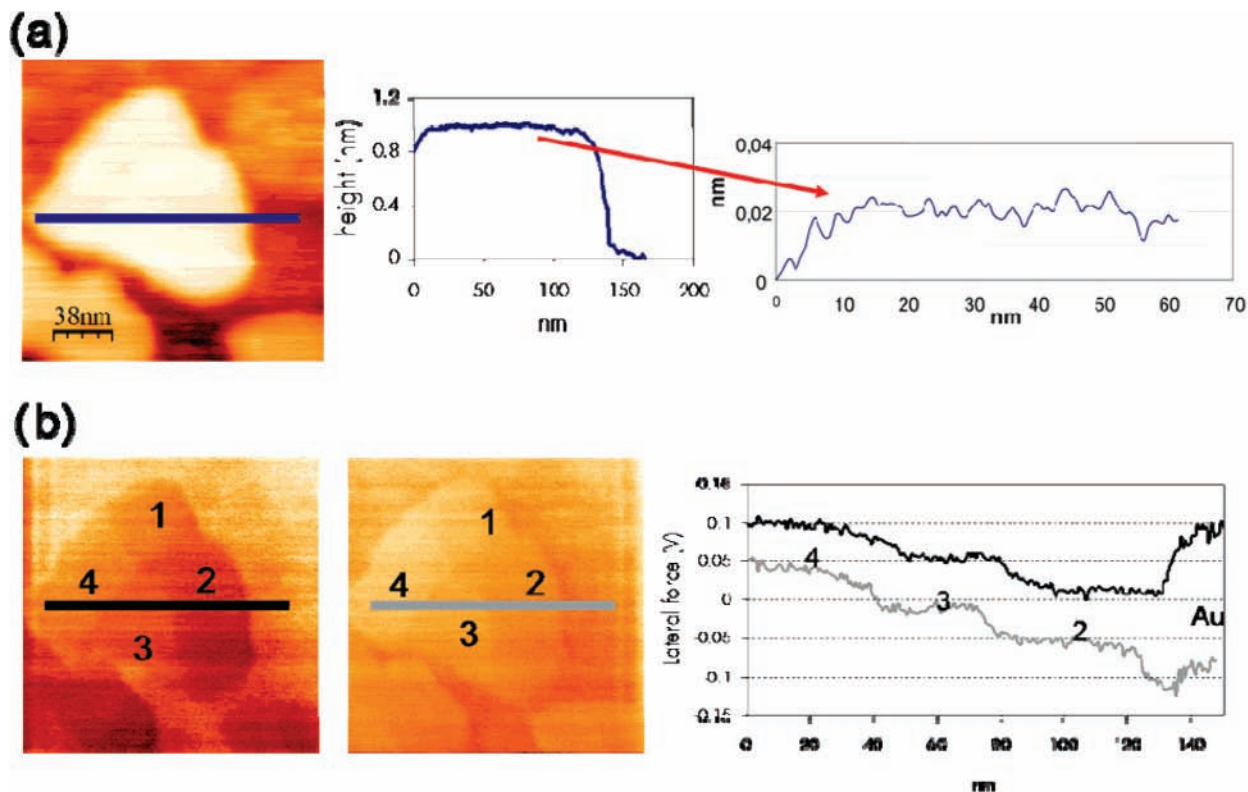


Figure 4. (a) Topographic SFM image showing one island of a C12 annealed sample. The line profile crossing the island shows a uniform height (± 0.03 nm) along it, better seen in the close-up profile. (b) Simultaneously measured forward (left) and backward (medium) lateral force images. Four domains exhibiting different lateral force contrast are observed. Right: lateral force profiles along the lines marked in the corresponding images, crossing domains numbers 2, 3, and 4 as well as the gold substrate, used as reference.

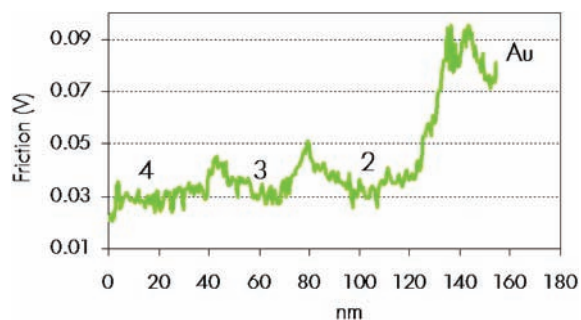


Figure 5. (a) Friction plot calculated from the forward and backward profiles marked in the lateral force images of Figure 4. The friction force is defined as $1/2(F_f^t - F_b^t)$. Except at the boundaries of the domains (where friction increases due to the mismatch between the forward and the backward images), all molecular domains exhibit roughly the same friction value, which is otherwise considerably lower than that measured on the gold substrate.

response, within the experimental error, and considerably lower than that obtained in the bare gold. We note that equal friction values were otherwise expected from structurally equivalent domains where the packing density, main contribution to total friction values, is identical and where no lateral packing anisotropy exists.

These results are strong evidence of how, even in those cases where lattice-resolved SFM imaging is not useful to discern between rotational domains, friction asymmetry determination permits deciphering structural domains presenting the same 2D hexagonal symmetry but where differences in the molecular tilt angle direction exist. A similar effect ascribed to the coexistence of domains with different molecular tilt directions was observed by SFM in several microns large thiolipid islands.²⁶ This is, however, the first time that this asymmetry has been observed

in alkanethiol samples, in which the domains are 1 order of magnitude smaller (hundreds of nanometers).

On the basis of our results and by analogy to those reported by Liley and co-workers, we conclude that the domains observed correspond to equivalent 2D hexagonal regions presenting different tilt directions and which coexist within the same island after coalescence promoted by a relatively fast (20 min) postannealing procedure of the C12 samples. We note that, however, large single-domains islands can be obtained when island growth proceeds during long periods of time (hours) at ambient temperature,⁴² which permits molecular aggregation and rearrangement as expected for a growth under closer to equilibrium conditions.

Conclusions

By means of friction force microscopy (FFM), we have resolved, for the first time, different domains within alkanethiol islands self-assembled on Au(111). Depending on the particular 2D arrangement of the molecules, either lattice-resolved SFM imaging or high sensitivity lateral force imaging has been employed to distinguish between equivalent domains. In islands presenting the $(2 \times \sqrt{3})$ rect configuration, the lack of invariance under rotation of the rectangular space group symmetry allows resolving the coexistence of equivalent, rotated, domains within an island from lattice-resolved images along the domain boundaries. Lattice-resolved images also acquired in the bare gold areas of the terraces where the island is located serve as an in-situ reference to accurately model the relative orientation and lattice spacing of each molecular domain.

In islands presenting the $(\sqrt{3} \times \sqrt{3})R30^\circ$ hexagonal configuration, because of its 2D rotational invariance, equivalent domains cannot be distinguished from lattice-resolved images. In this case, we have shown that the high sensitivity afforded

in lateral force images can be used. Whereas topographic images show flat islands with uniform heights, lateral force images reveal the coexistence of domains within a given island, presenting a different lateral force contrast (i.e., friction asymmetry) but the same absolute friction values (i.e., no friction anisotropy). The friction asymmetry is caused by domains presenting a different relative orientation between the molecular tilt direction and the tip scanning direction; this influences the lateral torsion of the cantilever in a measurable way. It is worth mentioning that these multidomain islands have only been observed when, after substrate withdrawal from the alkanethiol solution, samples are annealed during 20 min at 70 °C. On the contrary, when the diffusion process is allowed to proceed at ambient temperature, single-domain islands, presenting a homogeneous friction contrast, are obtained.

Acknowledgment. The authors grateful appreciate the continuous and enthusiastic support of Professor Giacinto Scoles during the years of sharing scientific interests. We acknowledge the EU for financial support under Contract No. NMP4-CT-2006-032109 as well as the Spanish MEC through Grants MAT2004-20291-E and MAT2007-62732.

References and Notes

- Hardy, W. *Proc. R. Soc. London, Ser. A* **1912**, 86, 610.
- Binnig, G.; Quate, C. F.; Gerber, C. H. *Phys. Rev. Lett.* **1986**, 56, 930.
- Xiao, X.; Hu, J.; Charych, D. H.; Salmeron, M. *Langmuir* **1996**, 12, 235.
- Carpick, R. W.; Salmeron, M. *Chem. Rev.* **1997**, 97, 1163.
- Lio, A.; Charych, D. H.; Salmeron, M. *J. Phys. Chem. B* **1997**, 101, 3800.
- Lio, A.; Morant, C.; Ogletree, D. F.; Salmeron, M. *J. Phys. Chem. B* **1997**, 101, 4767.
- McDermott, M. T.; Green, J.-B. D.; Porter, M. D. *Langmuir* **1997**, 13, 2504.
- Barrena, E.; Kopta, S.; Ogletree, D. F.; Charych, D. H.; Salmeron, M. *Phys. Rev. Lett.* **1999**, 82, 2880.
- Barrena, E.; Ocal, C.; Salmeron, M. *J. Chem. Phys.* **2000**, 113, 2413.
- Lee, S.; Shon, Y. S.; Colorado, R.; Guenard, R. L.; Lee, T. R.; Perry, S. S. *Langmuir* **2000**, 16, 2220.
- Barrena, E.; Ocal, C.; Salmeron, M. *Surf. Sci.* **2001**, 482, 1216.
- Perry, S. S.; Lee, S.; Shon, Y.-S.; Colorado, R., Jr.; Lee, T. R. *Trib. Lett.* **2001**, 10, 81.
- Zhang, C.; Liang, Q.; Wang, B.; Xiao, X. *J. Appl. Phys.* **2004**, 95, 3411.
- Li, L.; Yu, K.; Jiang, S. *J. Phys. Chem. B* **1999**, 103, 8290.
- Shon, Y.-S.; Lee, S.; Colorado, R., Jr.; Perry, S. S.; Lee, T. R. *J. Am. Chem. Soc.* **2000**, 122, 7556.
- Kim, H. I.; Graupe, M.; Oloba, O.; Koini, T.; Imaduddin, S.; Lee, T. R.; Perry, S. S. *Langmuir* **1999**, 15, 3179.
- Leggett, G. J.; Brewer, N. J.; Chong, K. S. L. *Phys. Chem. Chem. Phys.* **2005**, 7, 1107.
- Houston, J. E.; Doelling, C. M.; Vanderlick, T. K.; Hu, Y.; Scoles, G.; Wenzl, I.; Lee, T. R. *Langmuir* **2005**, 21, 3926.
- Brewer, N. J.; Foster, T. T.; Leggett, G. J.; Alexander, M. R.; McAlpine, E. *J. Phys. Chem. B* **2004**, 108, 4723.
- Salmeron, M. *Trib. Lett.* **2001**, 10, 69.
- van der Vegte, E. W.; Subbotin, A.; Hadziioannou, G. *Langmuir* **2000**, 16, 3249.
- Morita, S. *Surf. Sci. Rep.* **1996**, 23, 1.
- Chen, J.; Ratera, I.; Murphy, A.; Ogletree, D. F.; Fréchet, J. M. J.; Salmeron, M. *Surf. Sci.* **2006**, 600, 4008.
- Santesson, L.; Wong, T. M. H.; Taborelli, M.; Descouts, P.; Liley, M.; Duschl, C.; Vogel, H. *J. Phys. Chem.* **1995**, 99, 1038.
- Gourdon, D.; Burnham, N. A.; Kulik, A.; Dupas, E.; Oulevey, F.; Gremaud, G.; Stamou, D.; Liley, M.; Dienes, Z.; Vogel, H.; Duschl, C. *Trib. Lett.* **1997**, 3, 317.
- Liley, M.; Gourdon, D.; Stamou, D.; Meseth, U.; Fischer, T. M.; Lautz, C.; Stahlberg, H.; Vogel, H.; Burnham, N. A.; Duschl, C. *Science* **1998**, 280, 273.
- Carpick, R. W.; Sasaki, D. Y.; Burns, A. R. *Trib. Lett.* **1999**, 7, 79.
- Bluhm, H.; Schwars, U. D.; Meyer, K. P.; Wiesendanger, R. *Appl. Phys. A* **1995**, 61, 525.
- Ulman, A.; Eilers, J. E.; Tillman, N. *Langmuir* **1989**, 5, 1147.
- Nuzzo, R. G.; Dubois, L. H.; Allara, D. L. *J. Am. Chem. Soc.* **1990**, 112, 558.
- Fenter, P.; Eisenberger, P.; Liang, K. S. *Phys. Rev. Lett.* **1993**, 70, 2447.
- Camillone, N., III; Chidsey, C. E. D.; Liu, G. Y.; Scoles, G. *J. Chem. Phys.* **1993**, 98, 3503.
- Poirier, G. E.; Tarlov, M. J. *Langmuir* **1994**, 10, 2853.
- Delamarche, E.; Michel, B.; Gerber, C.; Anselmetti, D.; Guntherodt, H. J.; Wolf, H.; Ringsdorf, H. *Langmuir* **1994**, 10, 2869.
- Maksymovych, P.; Sorescu, D. C.; Yates, J. T., Jr. *Phys. Rev. Lett.* **2006**, 97, 146103.
- Yu, M.; Bovet, N.; Satterley, C. J.; Bengió, S.; Lovelock, K. R. J.; Milligan, P. K.; Jones, R. G.; Woodruff, D. P.; Dhanak, V. *Phys. Rev. Lett.* **2006**, 97, 166102.
- Mazzarello, R.; Cossaro, A.; Verdini, A.; Rousseau, R.; Casalis, L.; Danisman, M. F.; Floreano, L.; Scandolo, S.; Morgante, A.; Scoles, G. *Phys. Rev. Lett.* **2007**, 98, 016102.
- Barrena, E.; Ocal, C.; Salmeron, M. *J. Chem. Phys.* **1999**, 111, 9797.
- Barrena, E.; Ocal, C.; Salmeron, M. *J. Chem. Phys.* **2001**, 114, 4210.
- Barrena, E.; Palacios-Lidón, E.; Munuera, C.; Torrelles, X.; Ferrer, S.; Jonas, U.; Salmeron, M.; Ocal, C. *J. Am. Chem. Soc.* **2004**, 126, 385.
- Munuera, C.; Barrena, E.; Ocal, C. *Langmuir* **2005**, 21, 8270.
- Munuera, C.; Ocal, C. *J. Chem. Phys.* **2006**, 124, 206102.
- Kolbe, W. F.; Ogletree, D. F.; Salmeron, M. *Ultramicroscopy* **1992**, 42–44, 1113.
- Nanotec Electronica, E-28760 Tres Cantos, www.nanotec.es (accessed July 2007).
- Torrelles, X.; Barrena, E.; Munuera, C.; Rius, J.; Ferrer, S.; Ocal, C. *Langmuir* **2004**, 20, 9396.